J Mater Sci (2012) 47:397–402
DOI 10.1007/s10853-011-5811-2

Phase transition, dielectric and piezoelectric properties of $K_{0.5}Na_{0.5}NbO_3$–$CaTi_{0.9}Zr_{0.1}O_3$ lead-free ceramics

Dunmin Lin · Kin Wing Kwok

Received: 6 May 2011 / Accepted: 20 July 2011 / Published online: 29 July 2011

Abstract Lead-free $(1 - x)K_{0.5}Na_{0.5}NbO_3$–$xCaTi_{0.9}Zr_{0.1}O_3 + 0.75$ mol%MnO_2 piezoelectric ceramics have been prepared by an ordinary sintering technique and their phase transition, dielectric and piezoelectric properties have been studied. The results of X-ray diffraction show that $CaTi_{0.9}Zr_{0.1}O_3$ diffuse into $K_{0.5}Na_{0.5}NbO_3$ lattices to form a solid solution with a perovskite structure. After the addition of $CaTi_{0.9}Zr_{0.1}O_3$, both the cubic–tetragonal and tetragonal–orthorhombic phase transition temperatures decrease, and a relaxor behavior is induced. Coexistence of the orthorhombic and tetragonal phases is formed in the ceramics with $0.03 < x < 0.07$ at room temperature. Owing to the higher number of possible polarization states resulting from the coexistence of the two phases, the piezoelectric properties of the ceramics are enhanced significantly. The ceramic with $x = 0.05$ exhibits the following optimum properties: $d_{33} = 203$ pC/N, $k_p = 45.0\%$, and $T_C = 342$ °C.

Introduction

Lead zirconate titanate (PZT) and PZT-based ceramics with a perovskite structure have been widely used in actuators, sensors as well as microelectronic devices due to their superior piezoelectric and ferroelectric properties. However, the use of the lead-containing ceramics is a potential source of environmental problems because of the high toxicity of lead oxide. Therefore, there is a need to develop lead-free ferroelectric and piezoelectric ceramics with good piezoelectric properties for replacing the lead-containing ceramics in various applications.

$K_{0.5}Na_{0.5}NbO_3$ (KNN) has been considered one of the most promising candidates for lead-free piezoelectric ceramics as it possesses a high Curie temperature (~420 °C) and good ferroelectric properties ($P_r = 33$ μC/cm^2) [1, 2]. However, because of the high volatility of alkali elements at high temperatures, it is difficult to obtain dense and well-sintered KNN ceramics using a conventional sintering process. As a result, an air-fired KNN ceramic usually possess weakened piezoelectric properties, giving a low piezoelectric coefficient ($d_{33} = 80$ pC/N) and a low planar electromechanical coupling factor ($k_p = 36\%$) [2]. For a well-sintered KNN ceramic (e.g., prepared by a hot-pressing technique), $d_{33} = 160$ pC/N and $k_p = 45\%$ [1]. A number of studies have been carried out to improve the sinterability and piezoelectric properties of KNN-based ceramics; these include the formation of solid solutions of KNN with ABO_3-type compounds, such as KNN–$LiTaO_3$ [3], KNN–$Bi_{0.5}Na_{0.5}TiO_3$ [4], KNN–$SrTiO_3$ [5], KNN–$LiSbO_3$ [6], KNN–$BaTiO_3$ [7], KNN–$LiNbO_3$ [8], KNN–$BiAlO_3$ [9], and KNN–Li(Nb,Ta,Sb)O_3 [10], and the use of sintering aids, e.g., MnO_2 [11] and $K_{5.4}Cu_{1.3}Ta_{10}O_{29}$ [12]. It has been noted that the key approach for improving the piezoelectric properties of KNN-based ceramics is to lower the ferroelectric tetragonal–ferroelectric orthorhombic phase transition (T_{O-T}), forming coexistence of the tetragonal and orthorhombic phases at room temperature. Recently, a solid solution $0.5Ba(Zr_{0.2}Ti_{0.8})O_3$–$0.5(Ba_{0.7}Ca_{0.3})TiO_3$ with excellent piezoelectric properties

D. Lin · K. W. Kwok
Department of Applied Physics and Materials Research Centre, The Hong Kong Polytechnic University, Kowloon, Hong Kong, China

D. Lin (✉)
College of Chemistry and Materials Science, and Visual Computing and Virtual Reality Key Laboratory of Sichuan Province, Sichuan Normal University, Chengdu 610066, People's Republic of China
e-mail: ddmd222@yahoo.com.cn

has been developed [13]. It may be considered as $BaTiO_3$ modified with Ca^{2+} and Zr^{4+} ions. It can be also noted that $0.5Ba(Zr_{0.2}Ti_{0.8})O_3$–$0.5(Ba_{0.7}Ca_{0.3})TiO_3$ (that is, $Ba_{0.85}Ca_{0.15}(Ti_{0.90}Zr_{0.10})O_3$) solid solution has a Ti:Zr ratio of 9:1. On the other hand, $Ba(Ti_{1-x}Zr_x)O_3$ ceramics has a d_{33} of 236 pC/N[14]. After the introduction of Ca^{2+} into Ba $(Ti_{1-x}Zr_x)O_3$, the ceramics possess improved piezoelectric properties [13, 14]. Therefore, in this work, we add ABO_3-type $CaTi_{0.9}Zr_{0.1}O_3$ perovskite to $K_{0.5}Na_{0.5}NbO_3$ ferroelectric and aim at preparing $(1-x)K_{0.5}Na_{0.5}NbO_3$–$xCaTi_{0.9}Zr_{0.1}O_3$ lead-free ceramics so as to improve the piezoelectric properties of the ceramics. On the basis of our previous work [11], 0.75 mol% MnO_2 is added as a sintering aid in order to improve the densification of the ceramics.

Experimental

$(1-x)K_{0.5}Na_{0.5}NbO_3$–$xCaTi_{0.9}Zr_{0.1}O_3$ + 0.75 mol% MnO_2 ceramics (abbreviated as KNN–CTZ-x) were prepared by a conventional ceramic technique using analytical-grade metal oxides and carbonate powders: K_2CO_3 (99.9%), Na_2CO_3 (99.8%), $CaCO_3$ (99%), ZrO_2 (99%), TiO_2 (99.9%), Nb_2O_5 (99.95%), and MnO_2 (99%). The powders in the stoichiometric ratio of $(1-x)K_{0.5}Na_{0.5}NbO_3$–$xCaTi_{0.9}Zr_{0.1}O_3$ were first mixed thoroughly in ethanol using zirconia balls for 8 h. After the calcination at 850 °C for 6 h, 0.75 mol% of MnO_2 powders was added. The mixture was ball-milled again for 8 h, mixed thoroughly with a poly(vinyl alcohol) binder solution and then pressed into disk samples. After removal of the binder, the disk samples were sintered at 1110–1190 °C for 4 h in air. The diameter and thickness of the samples are 13 mm and 0.8, respectively. Silver electrodes were fired on the top and bottom surfaces of the samples at 650 °C for 10 min. The ceramics were poled under a dc field of 4–5 kV/mm at room temperature in a silicone oil bath for 30 min.

The crystalline structure of the sintered samples was examined using X-ray diffraction (XRD) analysis with CuK_α radiation (Bruker D8 Advance, Bruker AXS, Madison, WI). The microstructure was observed using a scanning electron microscopy (JEOL JSM-6400LV, JEOL, Japan). The bulk density ρ was measured by the Archimedes method. The relative permittivity ε_r and loss tangent $\tan\delta$ were measured as a function of temperature using an impedance analyzer (Agilent 4192A, Agilent Technologies Inc., Palo Alto, CA). A conventional Sawyer-Tower circuit was used to measure the polarization hysteresis (P–E) loop at 100 Hz. The electromechanical coupling factor k_p and frequency constant N_p were determined by the resonance method according to the IEEE Standards using an impedance analyzer (Agilent 4294A, Agilent Technologies Inc., Palo Alto, CA). The piezoelectric constant d_{33} was measured using a piezo-d33 meter (ZJ-3A, China, Institute of Acoustics, Chinese Academy of Sciences, Beijing, China).

Results and discussion

The XRD patterns of the KNN–CTZ-x ceramics are shown in Fig. 1. All the ceramics possess a pure perovskite structure and no secondary phase is observed. This suggests that a new solid solution of KNN with $CaTi_{0.9}Zr_{0.1}O_3$ is formed. As shown in the enlarged XRD patterns (Fig. 1b), the ceramics with $x \leq 0.03$ have an orthorhombic structure (space group: Bmm2; International Centre for Diffraction Data, JCPDS-ICDD Card no. 71-2171 (2001).) As x increases, a tetragonal phase appears and increases continuously. At $x \geq 0.7$, the ceramics possess the tetragonal phase only (space group: p4 mm; International Centre for Diffraction Data, JCPDS-ICDD Card no. 71-0945 (2001).) This suggests that coexistence of the orthorhombic and tetragonal phases is formed in the ceramics with $0.03 < x < 0.07$ at room temperature.

Figure 2 show the SEM micrographs of the KNN–CTZ-x ceramics with $x = 0$, 0.05 and 0.08. The ceramics are well-sintered and possess a high relative density (>96%). For each composition, the ceramics were sintered at different temperatures and their density was measured. The optimum sintering temperature was determined as the sintering temperature by which the ceramic had the largest density. It has been noted that the sintering temperature increases with increasing x. For the ceramic with $x = 0$, the optimum sintering temperature is 1100 °C, while those for

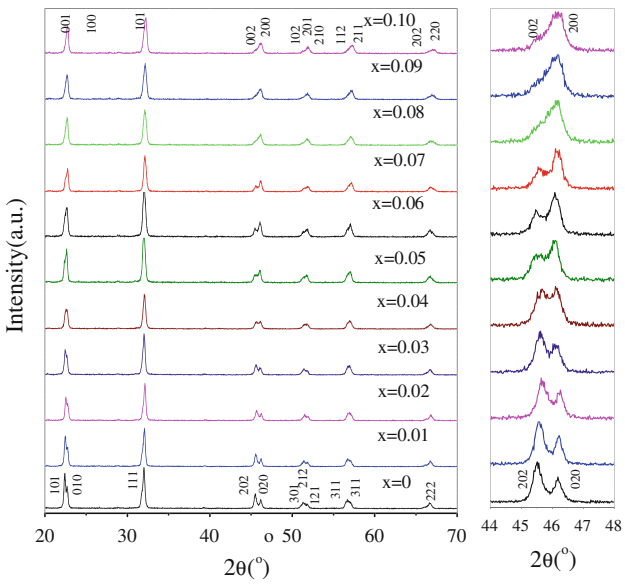

Fig. 1 X-ray diffraction patterns of the KNN–CTZ-x ceramics

the ceramics with $x = 0.05$ and 0.08 are 1160 and 1180 °C, respectively. This should be partly attributed to the high sintering temperature of calcium zirconate ceramics (≥1500 °C). Despite of the increase in the sintering temperature, the grain becomes smaller and more uniform with increasing x. As shown in Fig. 2a, the grains of the KNN–CTZ-0 ceramic are large, about 5 μm. However, as x increases to 0.05 and 0.08, the grain size decreases to about 1.2 and 0.7 μm, respectively. It has been shown that the addition of titanates with a perovskite structure to KNN ceramics usually leads to a reduction in the grain size [4, 9]. The KNN–CTZ ceramics have the bulk density values of 4.285–4.352 g/cm^3. On the basis of the XRD results for all the KNN–CTZ-x ceramics, the relatively densities are about 96–97% and have small dependence on x.

Figure 3 shows the temperature dependences of the relative permittivity ε_r at 10 kHz for the KNN–CTZ-x ceramics. As shown in Fig. 3a, the KNN–CTZ-0 ceramic exhibits the normal ferroelectric characteristic [1, 2], undergoing the cubic–tetragonal phase transition at 429 °C (T_C) and the tetragonal–orthorhombic phase transition at 207 °C (T_{O-T}). After the addition of $CaTi_{0.9}Zr_{0.1}O_3$, the ceramics with $x \leq 0.06$ exhibit similar temperature dependences of ε_r, but with different T_C and T_{O-T}. The tetragonal–orthorhombic phase transition peak becomes very weak for the ceramic with $x = 0.07$. For the ceramics with $x > 0.08$, only the cubic–tetragonal phase transition peak is observed in the temperature range of −150 to 500 °C. The variations of T_C and T_{O-T} with x for the ceramics are shown in Fig. 4. As x increases, both T_C and T_{O-T} decrease linearly at a rate of ~21 and ~27 °C/mol%, respectively. For the ceramic with $x = 0.05$, the observed T_{O-T} is 43 °C, which is close to room temperature, suggesting that the orthorhombic and tetragonal phases co-exist in the ceramic. This is in agreement with the results of X-ray diffraction (Fig. 1). In general, the phase

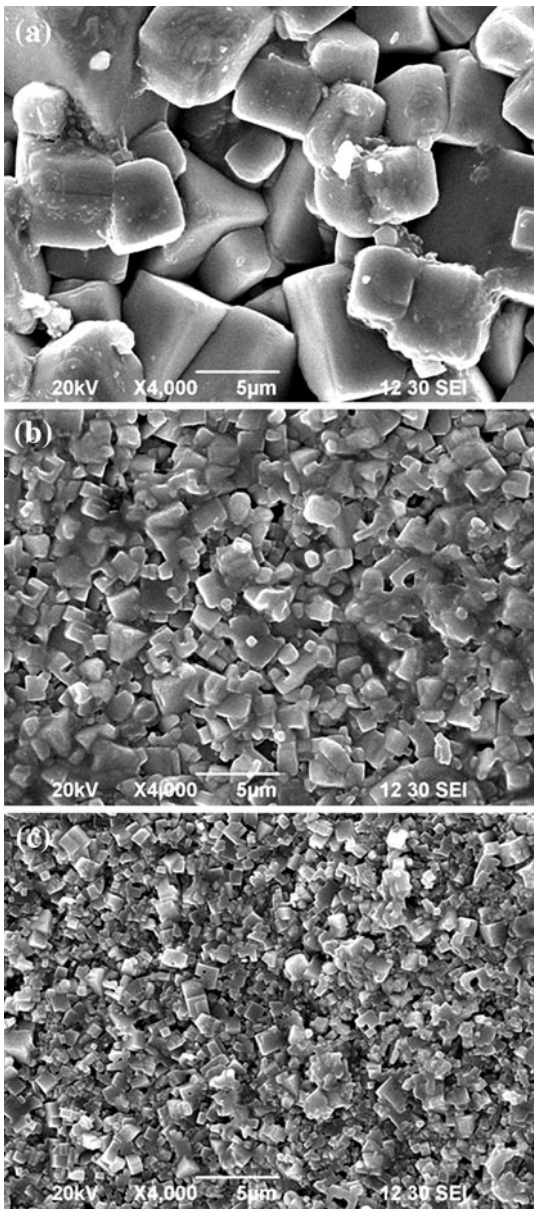

Fig. 2 SEM micrographs of the KNN–CTZ-x ceramics: **a** $x = 0$ sintered at 1110 °C for 4 h; **b** $x = 0.05$ sintered at 1160 °C for 4 h; and **c** $x = 0.08$ sintered at 1180 °C for 4 h

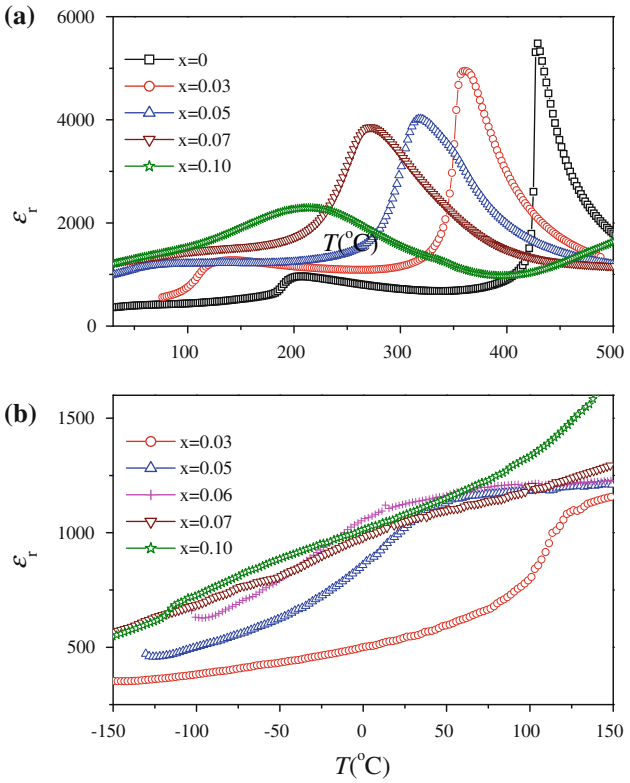

Fig. 3 Temperature dependences of the relative permittivity ε_r at 10 kHz for the KNN–CTZ-x ceramics in the temperature range of **a** from 25 to 500 °C and **b** from −150 to 150 °C

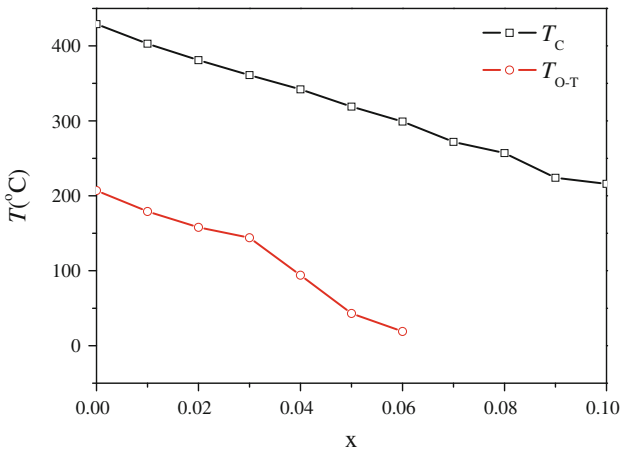

Fig. 4 Variations of the phase transition temperature T_C and T_{O-T} with x for the KNN–CTZ-x ceramics

transition temperatures of the KNN ceramics can be decreased by the substitution of Ta and Sb for Nb or the introduction of ABO_3-type perovskite titanates into the lattices. The reason is unclear and further investigation is needed to understand the phenomenon.

The temperature dependences of ε_r and tanδ at different frequencies (1 kHz, 10 kHz and 100 kHz) are shown in Fig. 5. It can be seen that the cubic–tetragonal phase transition peak for the KNN–CTZ-0 ceramic is sharp and frequency-independent, suggesting that the ceramic is a normal ferroelectric (Fig. 5a). As x increases, the transition peak becomes broadened and frequency dependent. For the ceramic with $x = 0.10$, the transition peak is very broad. These suggest that a diffuse phase transition is induced after the addition of $CaTi_{0.9}Zr_{0.1}O_3$ and the ceramics have transformed gradually from a normal ferroelectric to a relaxor ferroelectric.

The diffuseness of a phase transition can be determined by the modified Curie–Weiss law $1/\varepsilon_r - 1/\varepsilon_m = C^{-1}(T - T_m)^{\gamma}$ [15], where ε_m is the maximum value of relative permittivity at the phase transition temperature T_m, γ is the degree of diffuseness, and C is the Curie-like constant. γ can have a value ranging from 1 for a normal ferroelectric to 2 for an ideal relaxor ferroelectric. Based on the temperature plots of ε_r at 10 kHz, the graphs of $\ln(1/\varepsilon_r - 1/\varepsilon_m)$ versus $\ln(T - T_m)$ for the KNN–CTZ-x ceramics with $x = 0$, 0.05 and 0.10 were plotted, giving the results shown in Fig. 6. All the samples exhibit a linear relationship. By least-squared fitting the experimental data to the modified Curie–Weiss law, γ was determined. The calculated γ for the ceramic with $x = 0$ is 1.18, revealing the normal ferroelectric characteristics. As x increases, γ increases gradually to 1.62 at $x = 0.05$ and then to 1.91 at $x = 0.10$. This clearly shows that the ceramic has transformed gradually from a normal ferroelectric to a relaxor ferroelectric. The diffuse phase transition may arise from the increase in the disorder degree of A- and B-site ions after the partial substitutions of Ca^{2+} for the A-site Na^+ and K^+ and Ti^{4+} for the B-site Nb^{5+}.

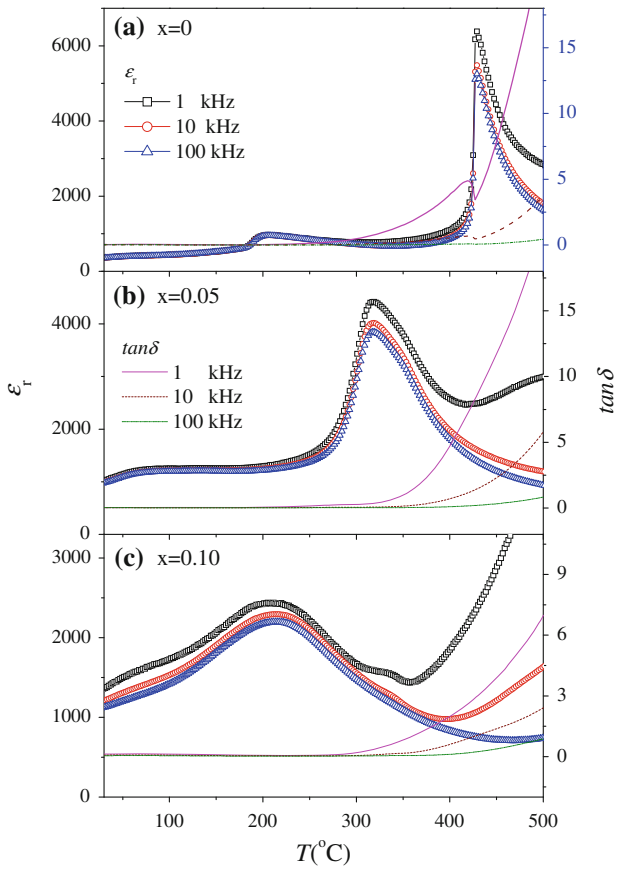

Fig. 5 Temperature dependences of the relative permittivity ε_r and loss tangent tanδ at 1, 10, and 100 kHz for the KNN–CTZ-x ceramics: **a** $x = 0$; **b** $x = 0.05$; and **c** $x = 0.10$

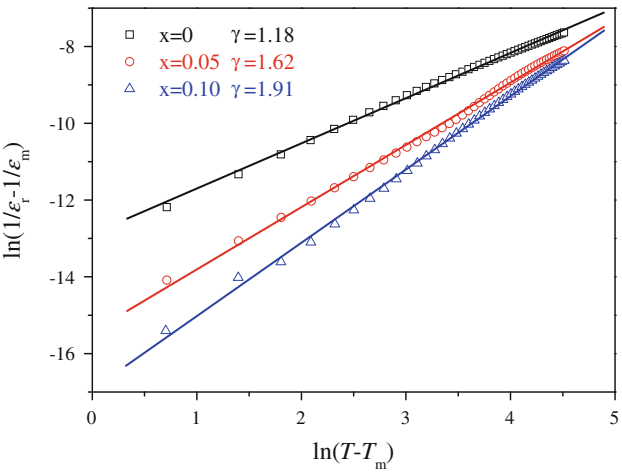

Fig. 6 Plots of $\ln(1/\varepsilon_r - 1/\varepsilon_m)$ versus $\ln(1/T - 1/T_m)$ for the KNN–CTZ-x ceramics with $x = 0$, 0.05, and 0.10. The *symbols* denote experimental data, while the *solid lines* denote the least-squared fitting line to the modified Curie–Weiss law

The *P–E* loops of the KNN–CTZ-*x* ceramics with $x = 0$, 0.05 and 0.10 are shown in Fig. 7a, while the variations of the remanent polarization P_r and coercive field E_c with *x* are shown in Fig. 7b. All the ceramics exhibit a typical *P–E* loop under an electric field of 5 kV/mm. The *P–E* loop of the KNN–CTZ-0 ceramic is square-like (Fig. 7a). As *x* increases, the *P–E* loop becomes flatted and slanted. As shown in Fig. 7b, the observed P_r increases slightly as x increases from 0.01 to 0.025 and then decreases rapidly, giving a maximum value of 23.8 μC/cm^2 at $x = 0.04$. The increase in P_r should be attributed to the more possible polarization states resulting from the coexistence of the orthorhombic and tetragonal phases. On the other hand, the observed E_c increases from 0.82 to 1.51 kV/mm as *x* increases from 0 to 0.10.

The variations of d_{33}, k_p, ε_r and tanδ with *x* for the KNN–CTZ-*x* ceramics are shown in Fig. 8. As shown in Fig. 8a, the observed d_{33} increases significantly with increasing x and then decreases, giving a maximum value of 203 pC/N at $x = 0.05$. The observed k_p increases slightly with increasing *x* and then decreases, showing the maximum value of 52.2% at $x = 0.03$. Unlike the piezoelectric properties, both the observed ε_r and tanδ increase with increasing *x*. As compared to a KNN ceramic (i.e., KNN–CTZ-0), the KNN–CTZ-*x* ceramics possess better piezoelectric properties, which should be attributed to the

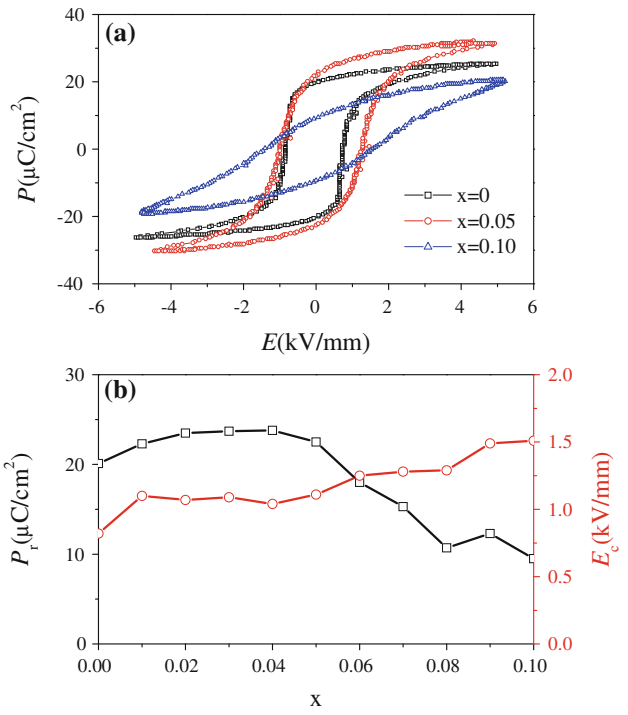

Fig. 7 **a** *P–E* hysteresis loops of the KNN–CTZ-*x* ceramics with $x = 0$, 0.05 and 0.10. **b** Variations of the remanent polarization P_r and coercive field E_c with *x* for the KNN–CTZ-*x* ceramics

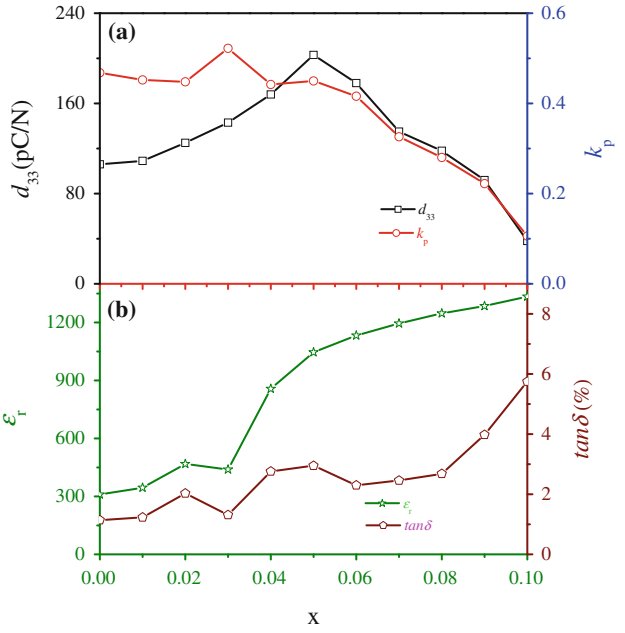

Fig. 8 Variations of d_{33}, k_p, k_t, ε_r, and tanδ with *x* for the KNN–CTZ-*x* ceramics

increase in the more possible polarization states resulting from the coexistence of the orthorhombic and tetragonal phases [16]. Similar results have been observed for other KNN-based ceramics. Table 1 compares the electrical properties of some KNN-based ceramics. In general, the effective approach to improve the piezoelectric properties of KNN-based ceramics is to lower the tetragonal–orthorhombic phase transition, forming coexistence of the tetragonal and orthorhombic phases at room temperature.

The thermal stability of the KNN–CTZ-*x* ceramics is an important issue for practical applications. Figure 9 show the variations of k_p and N_p with temperature for the KNN–CTZ-*x* ceramic with $x = 0.05$, which possesses the optimum piezoelectric and ferroelectric properties. It can be seen that the observed k_p has a weak temperature dependence in the temperature range from −50 to 150 °C. This should be attributed to the diffusive nature of the orthorhombic–tetragonal phase transition in a broad temperature as shown in Fig. 4b. Probably owing to the coexistence of two phases, the observed k_p reaches a maximum value of 45.0% at 35 °C which is close to the observed T_{O-T} (43 °C). Unlike k_p, the observed N_p decreases as the temperatures increases and then increases, reaching a minimum value of 3278 Hz m at 35 °C. It is known that N_p is mainly related to the elastic compliance s_{11}^E and density ρ (s_{11}^E is proportional to $1/(4N_p^2\rho$ with a good approximation) [21]. At the temperature near T_{O-T}, the mechanical stiffness and/or the bonding strength of ionic constituents in NbO_6 octahedra are changed, resulting in a increase in s_{11}^E and thus a decrease in N_p.

Table 1 Electrical properties of some KNN-based ceramics

Compositions	d_{33} (pC/N)	k_p (%)	T_{O-T} (°C)	T_C (°C)
$K_{0.44}Na_{0.52}Li_{0.04}Nb_{0.76}Ta_{0.20}Sb_{0.04}O_3$ [17]	259	42	–	~270
KNN–$K_{5.4}Cu_{1.3}Ta_{10}O_{29}$ [18]	–	41	185	395
0.948KNN–0.052$LiSbO_3$ [19]	265	50	35	368
KNN–$LiNbO_3$ [8]	235	42	–	~450
KNN–$Bi_{0.5}Na_{0.5}TiO_3$ [4]	195	43	–	375
MnO_2-doped KNN–$BaTiO_3$ [20]	194	41	–	–
0.95KNN–0.05CTZ–0.75 mol%MnO_2	203	45	43	342

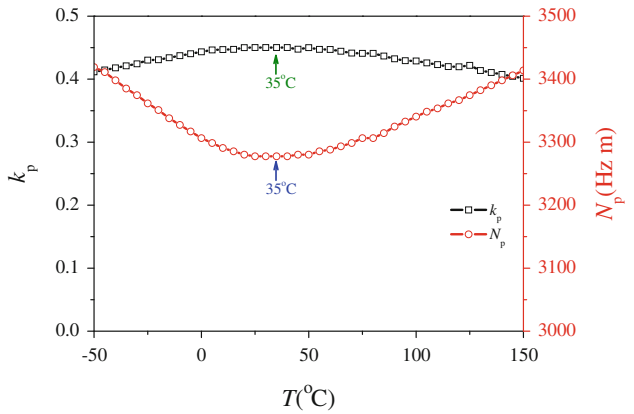

Fig. 9 Variations of k_p and N_p with temperature for the KNN–CTZ-0.05 ceramic

Conclusions

New lead-free $(1 - x)K_{0.5}Na_{0.5}NbO_3$–$xCaTi_{0.9}Zr_{0.1}O_3$ + 0.75 mol%MnO_2 piezoelectric ceramics have been prepared by an ordinary sintering technique. The ceramics possess a single-phase perovskite structure. The addition of $CaTi_{0.9}Zr_{0.1}O_3$ decreases both the cubic–tetragonal phase transition temperature (T_C) and the tetragonal–orthorhombic phase transition temperature (T_{O-T}) of the ceramics. It also makes the ceramics become more relaxor-like, showing a diffuse phase transition at T_C. Coexistence of the orthorhombic and tetragonal phases is formed at $0.03 < x < 0.07$ at room temperature, leading to a significant improvement of the piezoelectric properties. For the ceramic with $x = 0.05$, the piezoelectric properties become optimum: $d_{33} = 203$ pC/N, $k_p = 45.0\%$. Owing to the high T_C (342 °C), it also exhibits a good thermal stability.

Acknowledgements This work was supported by the Postdoctoral Fellowship grant (G-YX98) and the Centre for Smart Materials of The Hong Kong Polytechnic University.

References

1. Jaeger L, Egerton RE (1962) J Am Ceram Soc 45:209
2. Egerton L, Dillom DM (1959) J Am Ceram Soc 42(9):438
3. Guo Y, Kakimoto K, Ohsato H (2005) Mater Lett 59(2–3):241
4. Zuo R, Fang X, Ye C (2007) Appl Phys Lett 90:092904
5. Wang R, Xie R, Hanada K, Matsusak K, Bando H, Itoh M (2005) Phys Stat Sol 202(6):R57
6. Lin D, Kwok KW, Chan HLW (2007) J Appl Phys 101:074111
7. Park HY, Ahn CW, Song HC, Lee JH, Nahm S, Uchino K, Lee HG, Lee HJ (2006) Appl Phys Lett 89:062906
8. Guo Y, Kakimoto K, Ohsato H (2004) Appl Phys Lett 85(18):4121
9. Zuo R, Lv D, Fu J, Liu Y, Li L (2009) J Alloys Compd 476:836
10. Saito Y, Takao H, Tani T, Nonoyama T, Takatori K, Homma T, Nagaya T, Nakamur M (2004) Nature 432:84
11. Lin D, Kwok KW, Chan HLW (2007) J Am Ceram Soc 90:1458
12. Matsubara M, Yamaguchi T, Sakamoto W, Kikuta K, Yogo T, Hirano S (2005) J Am Ceram Soc 88:1190
13. Liu W, Ren X (2009) Phys Rev Lett 103:257602
14. Zhi Z, Ang C, Guo R, Bhalla AS (2002) J Appl Phys 92(3):1489
15. Uchino K, Nomura S, Cross LE, Tang SJ, Newnham RE (1980) J Appl Phys 51:1142
16. Jaffe B, Cook WR, Jaffe H (1971) Piezoelectric ceramics. Academic Press, London, p 135
17. Chang Y, Yang Z, Hou Y, Liu Z, Wang Z (2007) Appl Phys Lett 90:232905
18. Matsubara M, Yamaguchi T, Kikuta K, Hirano S (2005) Jpn J Appl Phys 44:6136
19. Zhang S, Xia R, Shrout TR, Zang G, Eang J (2008) J Appl Phys 100:104108
20. Ahn CW, Song HC, Nahm S, Park SH, Uchino K, Priya S, Lee HG, Kang NK (2006) Jpn J Appl Phys 44:L1361
21. IEEE standard on piezoelectricity, IEEE Std. 176-1987. The Institute of Electrical and Electronics Engineers, New York